CHAPTER IV
RESULTS AND DISCUSSION

4.1 PA 6/LDPE/Ionomer Ternary Blends

4.1.1 Differential Scanning Calorimetry

Tables 4.1 and 4.2 show the crystalline properties of the LDPE and PA 6 respectively as a function of ionomer compatibilizer content. In terms of the melting temperature (T_m), the addition of ionomer had little to no effect on the T_m of the LDPE. The T_m of pure ionomer was much lower than the T_m of LDPE, so one might have expected a drop in T_m of the LDPE in PA 6/LDPE blends. However, there was no decrease in the T_m of LDPE. Although no decrease in T_m, the weight fraction crystallinity of LDPE dropped dramatically as the weight percent of ionomer increased from 2.5 to 5.0. This was to be expected when the PA 6 content was high. In particular, for the PA 6/LDPE ratio of 80/20, the value of the weight fraction crystallinity became much closer to that of the pure ionomer, however no substantial change in T_m was observed. The change in weight fraction crystallinity with increasing ionomer content clearly indicates that the ionomer, as compatibilizer, substantially influences the crystallization behavior of LDPE. It is possible that the ethylene segments from the ionomer can co-crystallize with ethylene segments from the LDPE because there was no indication of a separate ionomer endotherm in the DSC thermograms of PA 6/LDPE blends.

For the crystalline properties of PA 6 in PA 6/LDPE blends, the T_m of PA 6 dropped slightly with decreasing PA 6 content. The addition of ionomer as compatibilizer had no effect on the T_m of PA 6 for the blends. However, the T_ms of PA 6 for all blend compositions were slightly lower than the T_m of pure PA 6. In addition, there was an increase in PA 6 crystallinity at low ionomer contents (0.1-1.0 % by weight). The weight fraction crystallinity of PA 6 showed no obvious trend and the scatter in the data was large so it was not possible to determine if the ionomer or LDPE had any affect on the PA 6 crystallinity.

Table 4.1 Crystalline properties of LDPE in PA 6/LDPE/ionomer ternary blends as determined by DSC

Surlyn® ionomer (%)	PA 6/LDPE Ratio							
	80/20		60/40		40/60		20/80	
	LDPE T_m(°C)	LDPE crystallinity (%)	LDPE T_m(°C)	LDPE crystallinity (%)	LDPE T_m(°C)	LDPE crystallinity (%)	LDPE T_m(°C)	LDPE crystallinity (%)
0.0	104.8	51.3	106.7	51.1	105.3	51.6	104.7	46.2
0.1	104.8	51.6	104.8	37.1	105.2	28.5	105.2	35.1
0.5	105.2	46.8	104.7	40.9	105.0	35.3	105.2	38.6
1.0	105.7	47.3	105.7	49.7	104.8	47.7	104.8	42.7
2.5	104.8	60.7	105.0	49.1	104.5	37.0	104.7	47.6
5.0	104.2	22.4	105.2	30.5	105.3	33.9	105.2	38.0
10.0	104.8	23.2	104.0	31.3	103.8	35.3	105.2	31.6
15.0	105.0	26.2	104.0	36.3	106.3	36.2	105.0	32.8
35.0	104.5	23.7	104.8	43.4	105.6	50.3	105.0	43.2

- Pure LDPE: T_m = 107.6 °C, Crystallinity (%) = 34.7
- Pure Surlyn® ionomer: T_m = 87.0 °C, Crystallinity (%) = 14.8

Table 4.2 Crystalline properties of PA 6 in PA 6/LDPE/ionomer ternary blends as determined by DSC

Surlyn® ionomer (%)	PA 6/LDPE Ratio							
	80/20		60/40		40/60		20/80	
	PA 6 T_m(°C)	PA 6 crystallinity (%)	PA 6 T_m(°C)	PA 6 crystallinity (%)	PA 6 T_m(°C)	PA 6 crystallinity (%)	PA 6 T_m(°C)	PA 6 crystallinity (%)
0.0	221.3	32.9	221.3	24.8	220.0	28.4	220.0	31.7
0.1	221.7	40.0	221.2	38.2	220.2	35.4	220.1	27.6
0.5	221.5	38.6	221.0	28.6	220.3	26.0	219.7	29.0
1.0	221.8	38.9	221.3	37.1	220.3	34.4	219.7	28.3
2.5	221.3	28.0	220.7	31.9	220.7	29.7	220.5	26.0
5.0	221.3	34.5	221.8	35.5	221.3	35.6	219.5	33.8
10.0	221.3	33.0	221.2	34.1	220.0	41.6	220.5	42.4
15.0	221.7	34.1	220.7	35.6	219.8	33.7	219.5	35.7
35.0	221.2	33.0	220.7	32.8	221.2	28.5	221.2	27.5

- Pure PA 6: T_m = 222.2 °C, Crystallinity (%) = 34.7
- Pure Surlyn® ionomer: T_m = 87.0 °C, Crystallinity (%) = 14.8

In a previous paper on binary blends of PA 6/ionomer (Willis *et al.*, 1993), the ionomer was shown to substantially slow down the rate of crystallization of the PA 6. In this current study, the kinetics have been probed indirectly since the cooling rate was kept constant for all materials. However, the cooling rate was quite slow compared to what one would get in a typical injection molding application for example, and this rather slow rate might mitigate any kinetic effects that could be present. The study did show, however, that the ionomer had a substantial effect on the crystallization behavior of the LDPE component of the PA 6/LDPE blends.

4.1.2 Dynamic Mechanical Analysis

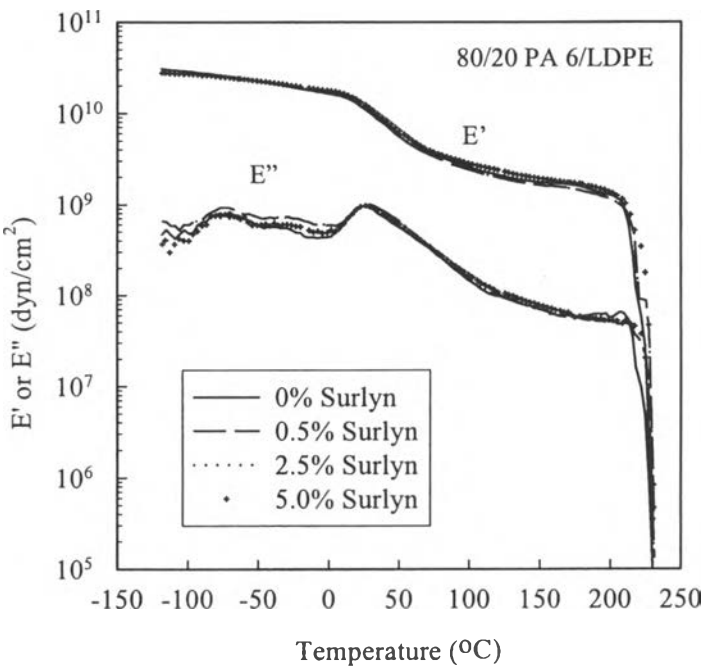

Figure 4.1 DMA spectra of samples with PA 6/LDPE ratio 80/20 at selected compatibilizer levels.

The DMA spectra for all samples are shown in Figures 4.1 to 4.5 in terms of the temperature dependence of storage modulus E' and loss modulus E". Figure 4.1 shows that the small-strain rheological properties (E' and E") for the system of highest PA 6 content (80 wt % PA 6) does not appear to change with ionomer content. However, when DMA was carried out at a E' value of 10^8 dyn/cm^2 the 80/20

PA 6/LDPE blends showed a marked increase in the drop-off temperature – the melting transition temperature – as the ionomer content was increased from 2.5 to 5.0 wt % (Table 4.3). The E' values for pure ionomer, pure LDPE and pure PA 6 are 70 °C, 99 °C and 218 °C respectively. The increase in drop-off E' modulus that occurs between ionomer contents of 2.5 and 5.0 wt % corresponds to the same weight fraction of 80/20 PA 6/LDPE as the drop-off in LDPE fractional crystallinity, which strongly suggested that both effects are real and due to the same phenomena. Since LDPE crystallites cannot directly influence the modulus at 220 °C (because the LDPE component will be in the molten state) it is suggested that the drop-off in crystallinity is a result of some complicated morphological change.

Table 4.3 Temperature at E' drop-off corresponding to the melting transition of the blends

Surlyn® ionomer (%)	Melting transition temperature (°C) of PA 6/LDPE blends			
	80/20[a]	60/40[a]	40/60[b]	20/80[a]
0.0	219	106	110	80
0.1	219	107	142	104.5
0.5	219	158.5	114	102
1.0	215	213	114	102
2.5	219.5	222	114	101
5.0	226	173	114	101
10.0	226	105	113	95.5
15.0	225.5	106	117	95.5
35.0	225.5	92.5	93	89

- Pure ionomer: melting transition temperature = 70 °C
- Pure LDPE: melting transition temperature = 99 °C
- Pure PA 6: melting transition temperature = 218 °C

[a] Temperature corresponding to E' of 10^8 dyn/cm^2

[b] Temperature corresponding to E' of 10^7 dyn/cm^2

Some of the melting transition temperatures listed in Table 4.3 are higher even than the pure PA 6 (218 °C); a direct comparison of the DMA spectra is shown in Figure 4.2. The increase in drop-off E' modulus of 80/20/5 PA 6/LDPE/ionomer compared with pure PA 6 is probably due to differences in the spatial arrangement of PA 6 crystallites in the sample since the DSC results indicate no substantial differences in T_m or percent crystallinity with the addition of compatibilizing agent.

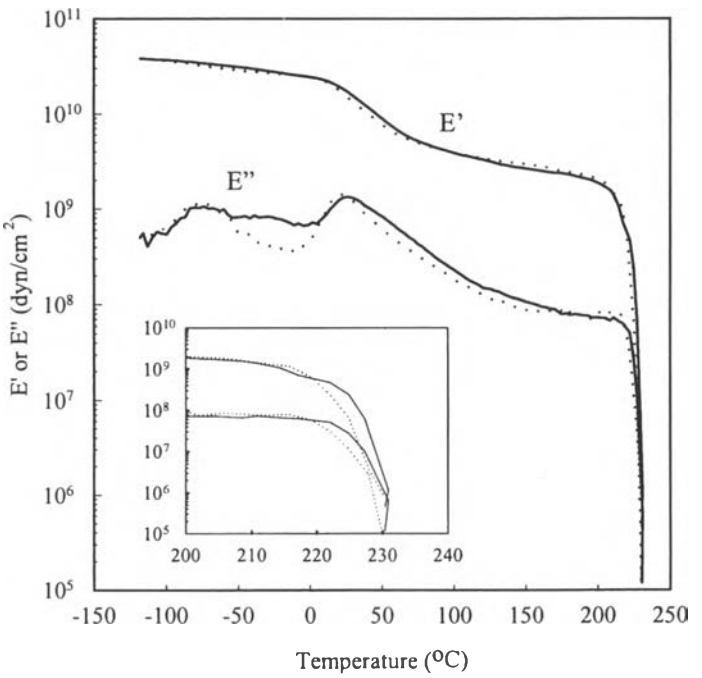

Figure 4.2 DMA spectra of pure PA 6 (dotted line) and a representative PA 6/ LDPE/ionomer blend sample (80/20/5, solid line) which shows higher storage modulus (E') in the melting transition region. The inset is shown to illustrate this phenomenon more clearly.

Figures 4.3 to 4.5 show much more dramatic changes in small-strain rheological properties (E' and E") than Figure 4.1. The addition of a small amount of ionomer substantially shifted the solid-liquid transition to higher melting temperatures, while even more ionomer caused a shift back towards lower melting temperatures. The change was most dramatic for the material with a PA 6/LDPE ratio of 60/40; originally the transition was near to that of pure polyethylene, it rose and approached the temperature of pure PA 6, and finally decreased to become even lower than that of the blend without ionomer. Clearly, the ionomer compatibilizer was causing phase inversion, first from a continuous LDPE phase to a continuous PA 6 phase, and then back once again to a continuous LDPE phase. Another interesting behavior was found for the low PA 6 content blends (blends containing 40 % and 20 % PA 6) where the addition of only 0.1 % ionomer produced the maximum shift in the melting transition to higher temperatures. It was strongly suspected that the above behaviors could be highly processing-condition dependent.

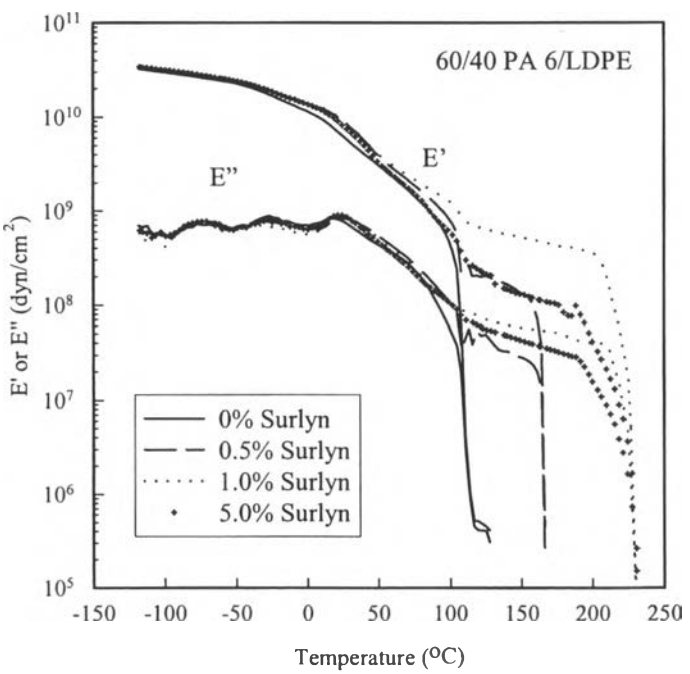

Figure 4.3 DMA spectra of samples with PA 6/LDPE ratio 60/40 at selected compatibilizer levels.

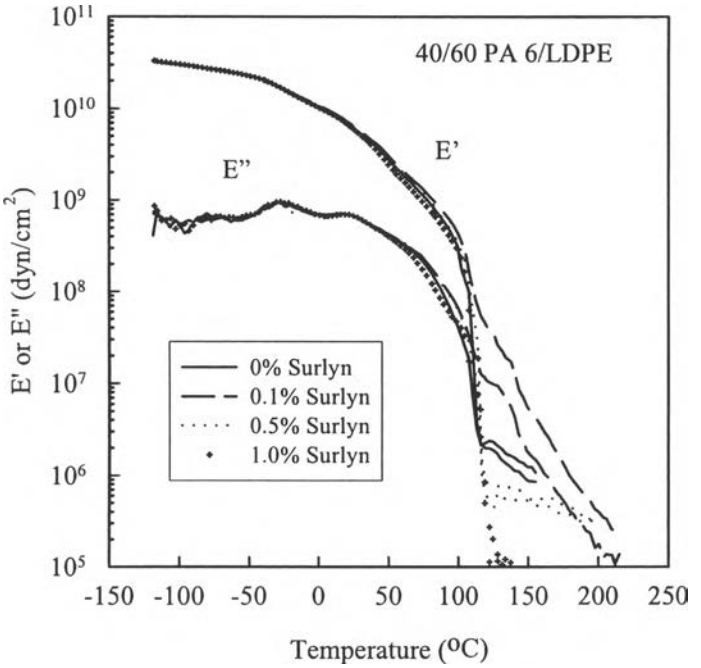

Figure 4.4 DMA spectra of samples with PA 6/LDPE ratio 40/60 at selected compatibilizer levels.

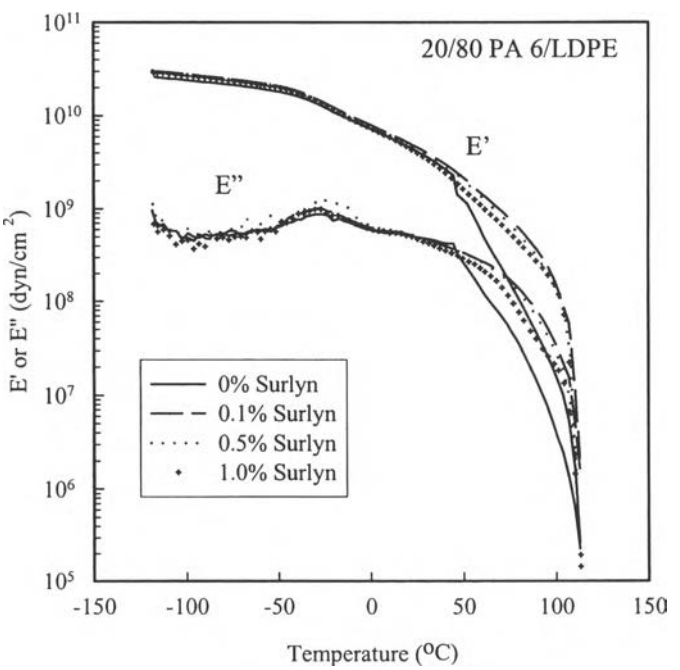

Figure 4.5 DMA spectra of samples with PA 6/LDPE ratio 20/80 at selected compatibilizer levels.

4.1.3 Mechanical Properties

4.1.3.1 Tensile Strength

The mechanical properties of pure PA 6, LDPE and ionomer are shown in Table 4.4. Table 4.4 and Figure 4.6 show that the tensile strength of all the blends were lower than that of pure PA 6. This could be attributed to the presence of particles of dispersed phase, which act as stress concentrators in the blends. The particles of dispersed phase could be introducing weak points in the materials, thus giving lower tensile strengths for the blends.

Table 4.4 Mechanical properties of pure PA 6, LDPE and ionomer

Pure materials	Tensile strength (MPa)	Elongation at break (%)
PA 6	73.8 ± 1.2	286.6 ± 26.1
LDPE	10.7 ± 0.2	95.3 ± 11.5
Ionomer	25.8 ± 0.5	474.4 ± 14.7

However, in the blends where LDPE was the major component, the tensile strengths were slightly higher than the pure LDPE. The tensile strengths of the blends were improved with the addition of ionomer between 0.1 and 5 wt %. It is proposed that the ionomer acted as an adhesive between the PA 6 and LDPE phases and this caused the size of the dispersed phase domains to decrease. These results are supported by SEM studies from a previous study (Rungravee, 2000). At ionomer contents above 5 wt %, the blends containing 60 %, 40 %, and 20 % PA 6 gave tensile strengths with very little or no change whereas the blends containing 80 % PA 6 gave a marked decrease in tensile strength. From these observations it is suggested that the particle size of the dispersed phase might have become stabilized. Thus the excess ionomer would tend to concentrate together and produce aggregates as the dispersed phase (Willis and Favis, 1985). In addition, it was observed that compatibilized blends of 80/20 PA 6/LDPE gave the highest tensile strength values.

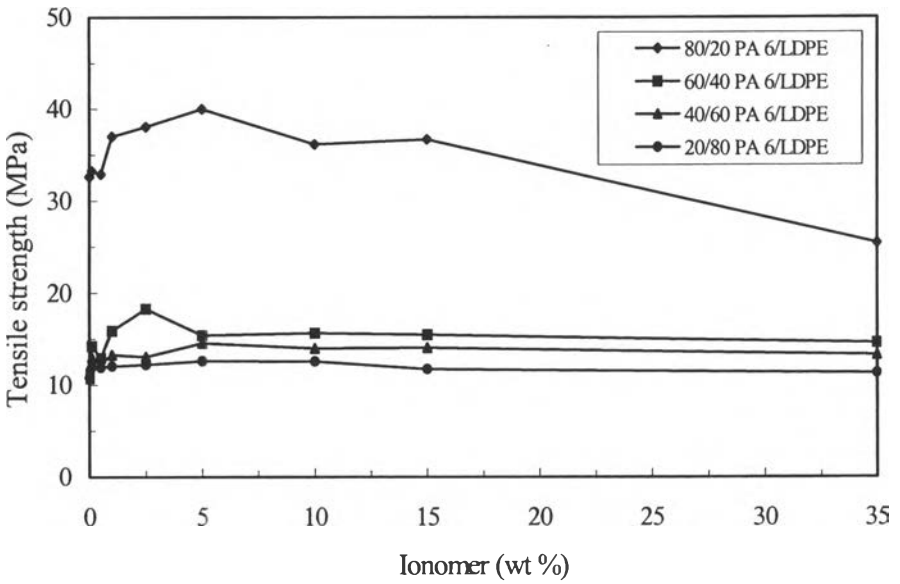

Figure 4.6 Tensile strength of PA 6/LDPE blends as a function of ionomer content.

4.1.3.2 Elongation at Break

Elongation at break (ε_b) of PA 6/LDPE blends as a function of ionomer content are shown in Figure 4.7. From Table 4.4 and Figure 4.7 it can be seen that all blends gave lower ε_b than the pure materials. This was ascribed to the presence of the particles of dispersed phase, resulting in blend heterogeneity and therefore, lower ε_b. However, the ε_b of the blends improved with the addition of ionomer as compatibilizer. For blends containing 60 %, 40 % and 20 % PA 6, adding only 1.0 wt % of ionomer into the blends increased the ε_b, and the ε_b gradually increased with increasing ionomer content. It is suggested that the ionomer acted as an adhesive between the PA 6 and LDPE phases and reduced stress concentrations around dispersed particles. Thus, higher homogeneity can be achieved with respect to uncompatibilized PA 6/LDPE blends.

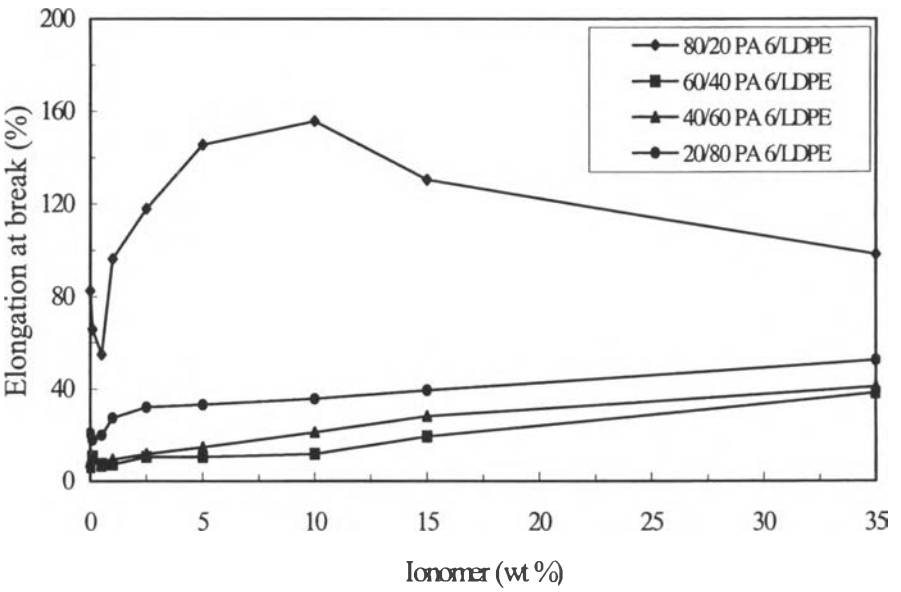

Figure 4.7 Elongation at break of PA 6/LDPE blends as a function of ionomer content.

For blends containing 80 % PA 6, ε_b of the compatibilized blends increased with when ionomer content from 1.0 % to 10 % but then dropped in ε_b between 10 and 35 wt % ionomer. It is proposed that aggregation of excess ionomer occurred and caused a reduction of homogeneity in the blends resulting in a lowering of ε_b. However, the compatibilized blends of 80/20 PA 6/LDPE all gave higher ε_b values than the other blends. This was attributed to the high value of ε_b for the pure PA 6 (286.6 %).

4.2 PA 6/Ionomer Binary Blends

4.2.1 Characterization of Blends

4.2.1.1 Specific Interactions

From all possible interactions that could occur when PA 6 is blended with Surlyn® ionomer, hydrogen bonding and chemical reactions at the interface are the most probable ones. A possible chemical reaction that could take place during melt mixing is amide formation between terminal amine groups of PA 6 and carboxylic acid groups of ionomer (Figure 4.8). This type of reaction has been previously proposed by MacKnight *et al.* (1985).

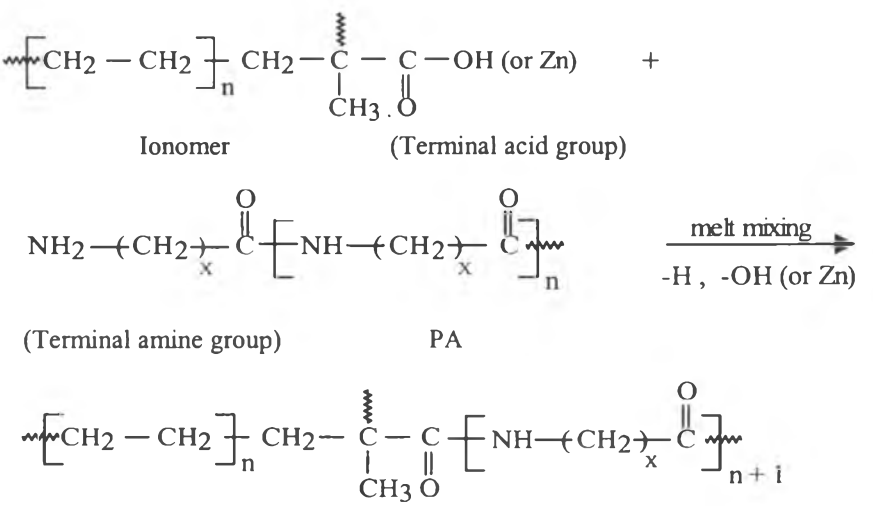

Figure 4.8 Proposed chemical reaction between terminal amine group of PA and carboxylic group of ionomer.

FTIR spectra for PA 6/ionomer blends are shown in Figure 4.9. For pure ionomer (Figure 4.9 g), the hydrogen bond carbonyl stretching frequency occurs at 1699 cm^{-1}. The peak at 1585 cm^{-1} corresponds to the antisymmetric stretching mode of the carboxylate groups present in the ion clusters (Willis *et al.*, 1993), and peaks at 2918 cm^{-1} and 2850 cm^{-1} represent C-H stretching. For pure PA 6 (Figure 4.9 a), the peak at 3300 cm^{-1} corresponds to N-H stretching. C-H stretching occurs at 2937 and 2868 cm^{-1}. Carbonyl stretching of PA 6 is at 1639 cm^{-1} and N-H bending is at 1544 cm^{-1}.

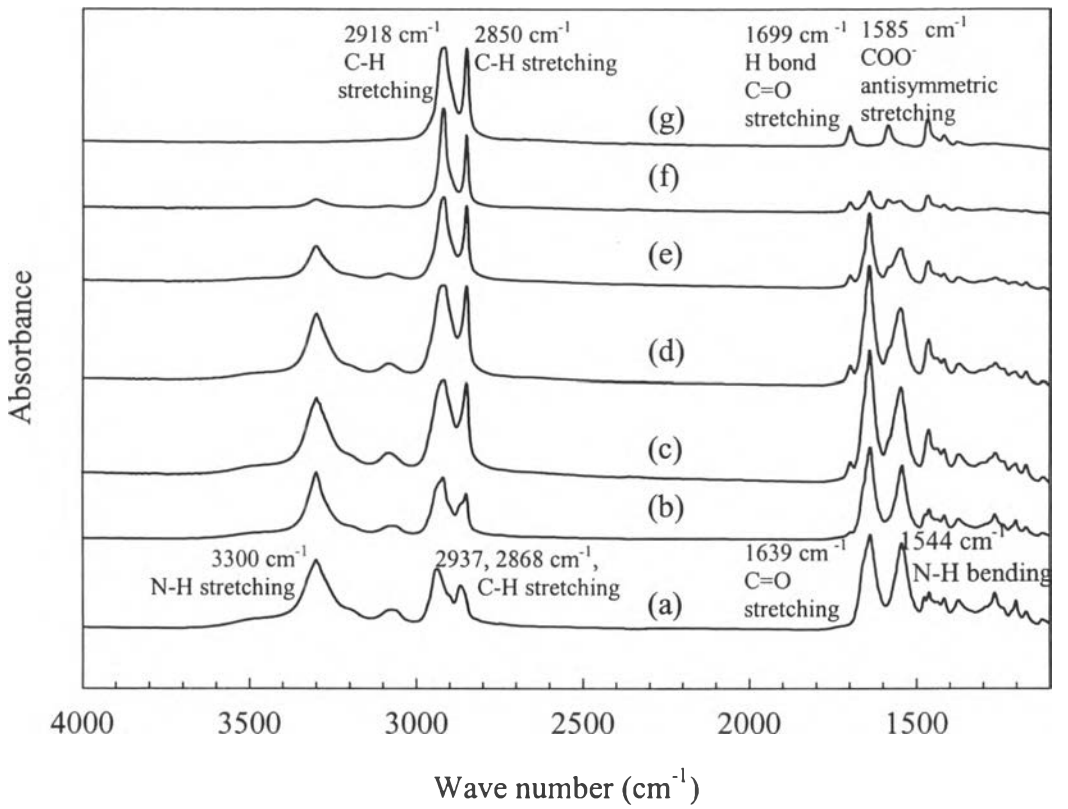

Figure 4.9 FTIR spectra of PA 6/Surlyn® ionomer blends: (a) 100/0, (b) 80/20, (c) 60/40, (d) 50/50, (e) 40/60, (f) 20/80, (g) 0/100.

For the PA 6/ionomer blends, spectra (b) to (f) showed absorbance peaks in the same positions as for pure PA 6 and pure ionomer at various intensities according to blend ratios. Thus, these FTIR spectra do not give clear evidence of copolymer formation because amide groups that would be observed for copolymer formation would also be present in the same peak position as the amide peak of pure PA 6.

To confirm that a chemical reaction had occurred, a "Molau test" was conducted according to the method of Molau (1965). To 0.1 g of the 80/20 PA 6/ ionomer blend was added 5 mL of 80 % formic acid. The mixture was shaken for 10 minutes and allowed to stand. The same procedure was used for the PA 6/LDPE blend. Figure 4.10 shows the results of the Molau test.

Several hours after the preparation of the mixtures, phase separation was observed in the 80/20 PA 6/LDPE blend (Figure 4.10 b). The lower

part of the solution consisted of formic acid and PA 6 dissolved in formic acid, and the upper part represented dispersed LDPE particles that did not dissolve in the formic acid. Turbidity persisted in the solution containing the 80/20 PA 6/ionomer blend, i.e. this was a positive Molau test (Figure 4.10 a). The highly turbid colloidal solution remained stable for several months. The material in the lower part of the solution represented a suspension of graft copolymer which was formed during melt mixing. Thus, it could be concluded that during the melt mixing, chemical reaction had occurred between the terminal amine groups of PA 6 and the carboxylic groups of ionomer, thus confirming the presence of copolymer.

Figure 4.10 Molau test solutions consisting of 80 % formic acid added to each of the following blends: (a) 80/20 PA 6/ionomer; (b) 80/20 PA 6/LDPE.

Evidence for possible hydrogen bonding that might have occurred in PA 6/ionomer blends are (i) the relative intensities of the ionomer carbonyl peaks (at 1699 cm^{-1}) and (ii) the peak width at half height, $W_{1/2}$, which normally increases with hydrogen bonding for the PA carbonyl peak at 1640 cm^{-1} (Willis *et al.*, 1993). It is possible for CO groups of PA to undergo hydrogen bonding with the OH groups of the ionomer. However since the intensities of the peaks for the blends varied according to blend composition, this suggests that these two carbonyl bands also did not give clear evidence of hydrogen bonding.

4.2.1.2 Morphological Studies

Scanning electron micrographs of fracture surfaces of PA 6/ ionomer blends are shown in Figure 4.11 (a-e). The morphologies of each composition appear to be homogeneous as it was difficult to observe the presence of any dispersed phase.

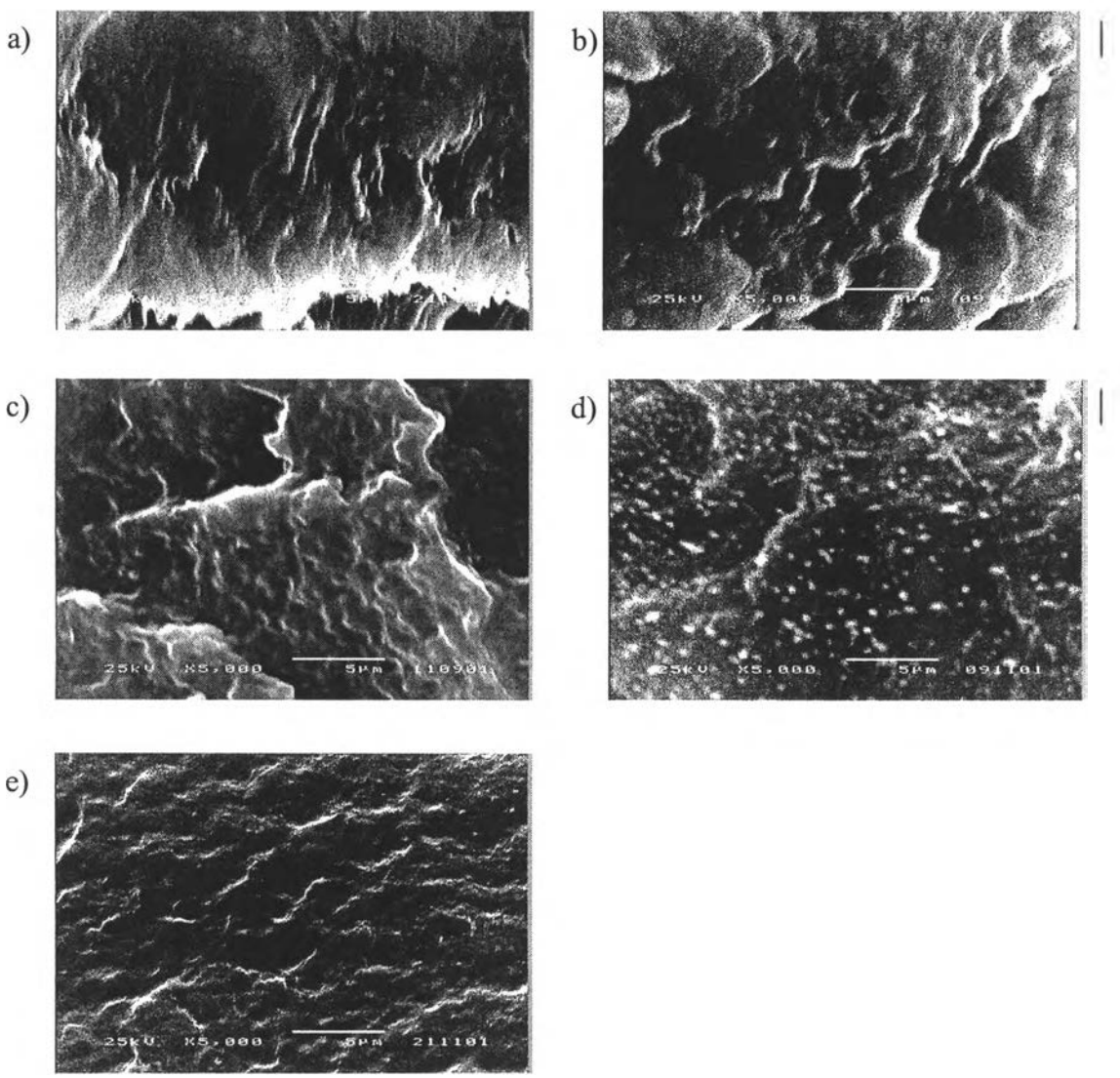

Figure 4.11 Scanning electron micrographs of fractured surfaces of PA 6/ionomer blends: a) 80/20, b) 60/40, c) 50/50, d) 40/60, e) 20/80.

However, when the fractured surfaces of blends containing 20 %, 40 %, and 50 % ionomer were etched by immersion in decalin (to remove the dispersed ionomer domain), and the fractured surfaces of blends containing 60 % and

80 % ionomer were etched by immersion in formic acid (to remove the dispersed PA 6 domain located at the surface) the dispersed phases were readily observed, as shown in Figure 4.12 (a-e).

The size of the dispersed ionomer and PA 6 domains were very small, approximately 1 μm, for all blend compositions. It is suggested that the PA 6/ ionomer graft copolymer formed during the blending process (by amidation reaction and hydrogen bonding) caused the sizes of the dispersed phase to be very small, and thus also enhance the compatibility of the PA 6/ionomer blends.

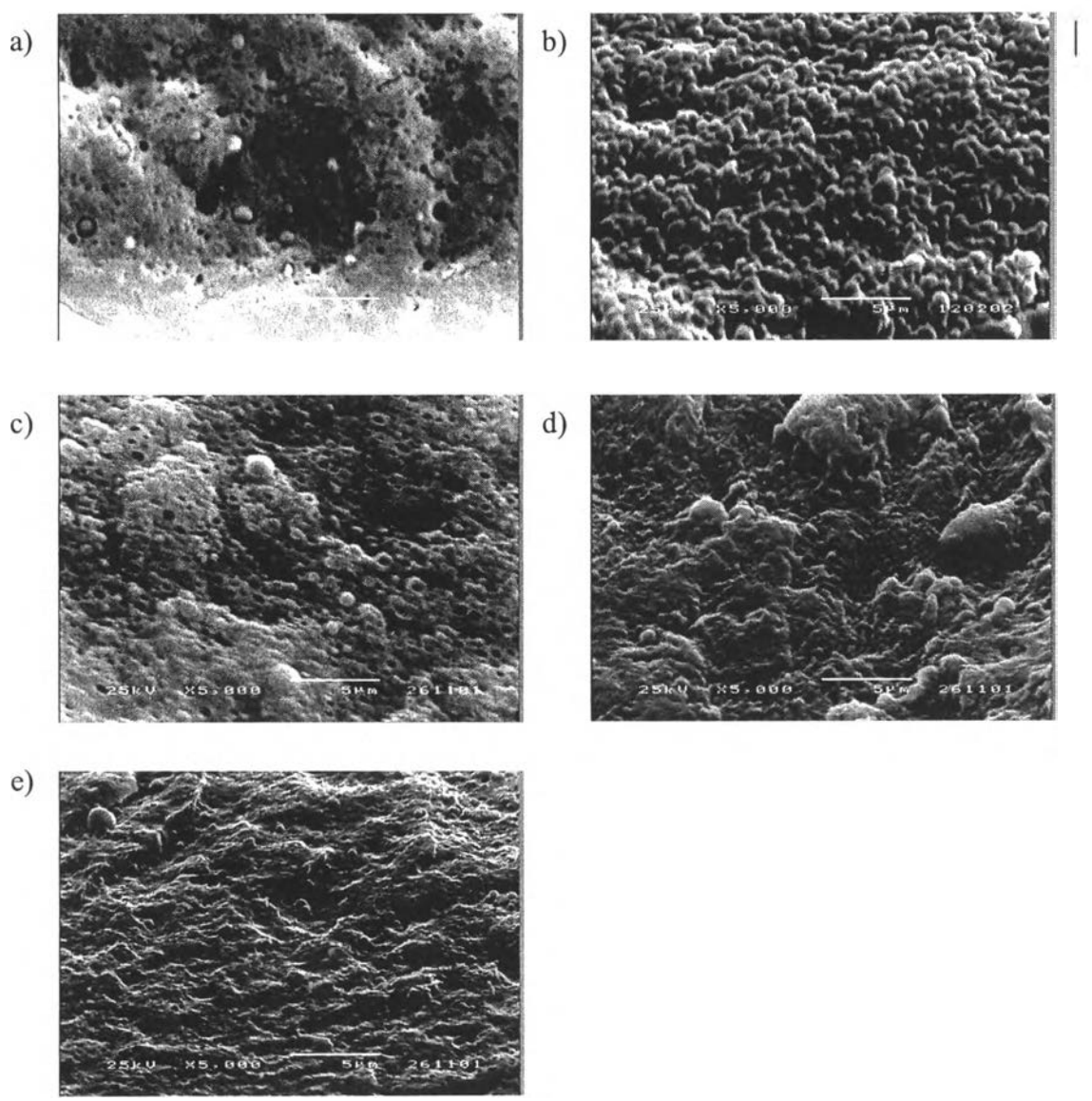

Figure 4.12 Scanning electron micrographs of fractured/etched surfaces of PA 6/ ionomer blends: a) 80/20, b) 60/40, c) 50/50, d) 40/60, e) 20/80.

However, because it was possible to observe the dispersed phases it was believed that the blends of PA 6/ionomer were immiscible. To confirm the immiscibility of PA 6/ionomer blends, dynamic mechanical analysis was used to investigate this point.

4.2.2 Dynamic Mechanical Analysis

DMA spectra for pure PA 6, pure ionomer and PA 6/ionomer blends are shown in Figure 4.13. The loss modulus E" was used as the basis for studying the relaxation behavior of polymer/polymer blends.

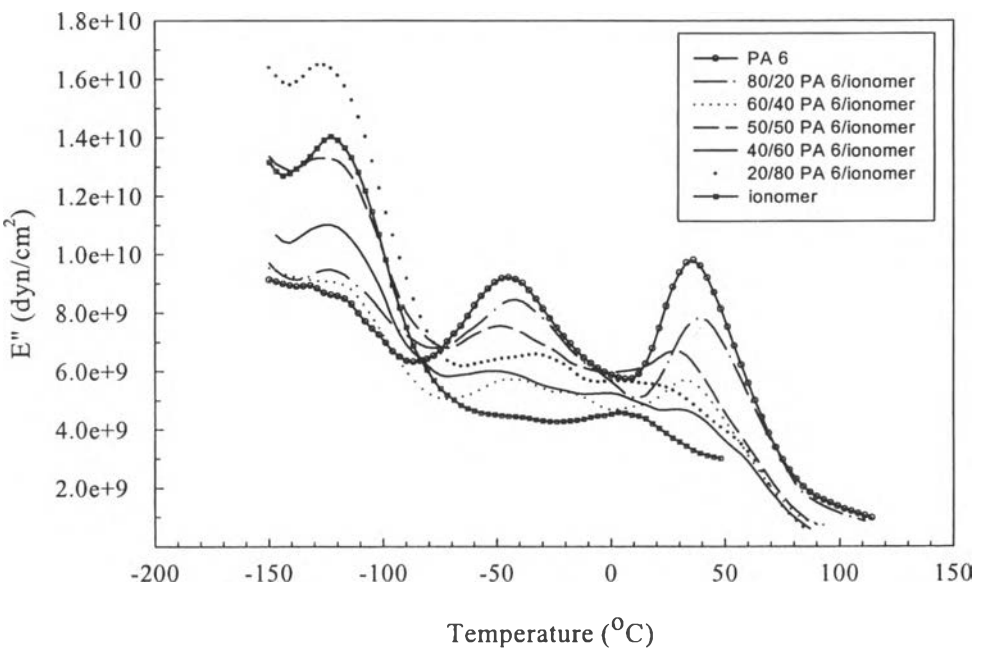

Figure 4.13 Temperature dependence of loss modulus, E", of pure PA 6, pure ionomer and PA 6/ionomer blends.

Three relaxation peaks for PA 6: α relaxation at 35.5 °C, β relaxation at - 45.8 °C and γ relaxation at -132.0 °C were observed. The α relaxation is believed to be associated with T_g, the β relaxation due to the segmental motion of the amide groups which are not bonded to other amide groups, and the γ relaxation is thought to be associated with the crankshaft rotation of the - $(CH_2)_n$ - groups in the main chain of the PA (Chuang and Han, 1985 and Kawagushi, 1959).

Pure Surlyn® ionomer exhibited two relaxation peaks: β' relaxation at 3 °C and γ relaxation at -123.0 °C. The β' relaxation is attributed to micro-Brownian segmental motion in the amorphous phase. The γ relaxation is ascribed to local molecular motion of the short segments in the amorphous phases (Tachino *et al.*, 1993). An α relaxation at 52 °C, which is generally attributed to a glass transition of Surlyn® ionomer, could not be observed in this study. However, because Surlyn® ionomer is a copolymer of ethylene and methacrylic acid, Sheng *et al.* (2000) believe that the relaxation peak at -123.0 °C is in fact the T_g, (the T_g of LDPE is -120 °C). Consequently, the exact T_g of Surlyn® ionomer is not clearly defined. However, the relaxation at -123.0 °C was considered to be the T_g of Surlyn® ionomer in this study. The relaxation peaks observed for the PA 6/ionomer blends are summarized in Table 4.5.

Table 4.5 Relaxation peak temperatures for PA 6/ionomer blends

Blend composition (PA 6/ionomer)	PA 6 peak		Surlyn® ionomer peak
	T_g (°C)	T_β (°C)	T_g (°C)
100/0	35.5	-45.8	-
80/20	38.5	-42.7	-124.3
60/40	32.2	-45.0	-123.0
50/50	28.1	-49.0	-126.0
40/60	27.0	-51.3	-124.7
20/80	21.0	-33.4	-127.4
0/100	-	-	-123.0

It is worth noting that for the PA 6/ionomer blends (i) the T_γ values for the PA 6 peaks could not be observed whereas the T_g values for the Surlyn® ionomer peaks shifted toward lower temperatures (from -123.0 °C to -127.4 °C), (ii) the T_g values for PA 6 peaks were depressed with increasing ionomer content but at 80/20 PA 6/ionomer the T_g value shifted to a higher temperature, (iii) the T_β values for PA 6 peaks were also shifted to both higher and lower temperatures by the presence

of ionomer. It is suggested that chemical reactions and hydrogen bonding occurred between the amorphous phases of PA 6 and ionomer and this caused the relaxation peaks to shift. The shifting of the relaxation peaks towards each other also implied some compatibility enhancement (Molnar and Eisenberg, 1993). Thus, the ionomer showed considerable compatibility enhancement with PA 6. However, since blends of PA 6/Surlyn® ionomer showed a series of relaxation peaks, it appears that PA 6/Surlyn® ionomer blends were immiscible.

4.2.3 Rheological Studies

4.2.3.1 Complex Viscosity

The complex viscosity, η^*, represents the viscosity of the material measured from mechanical oscillations within the linear viscoelastic regime. Figure 4.14 shows η^* as a function of frequency for pure PA 6, pure ionomer and PA 6/ ionomer blends.

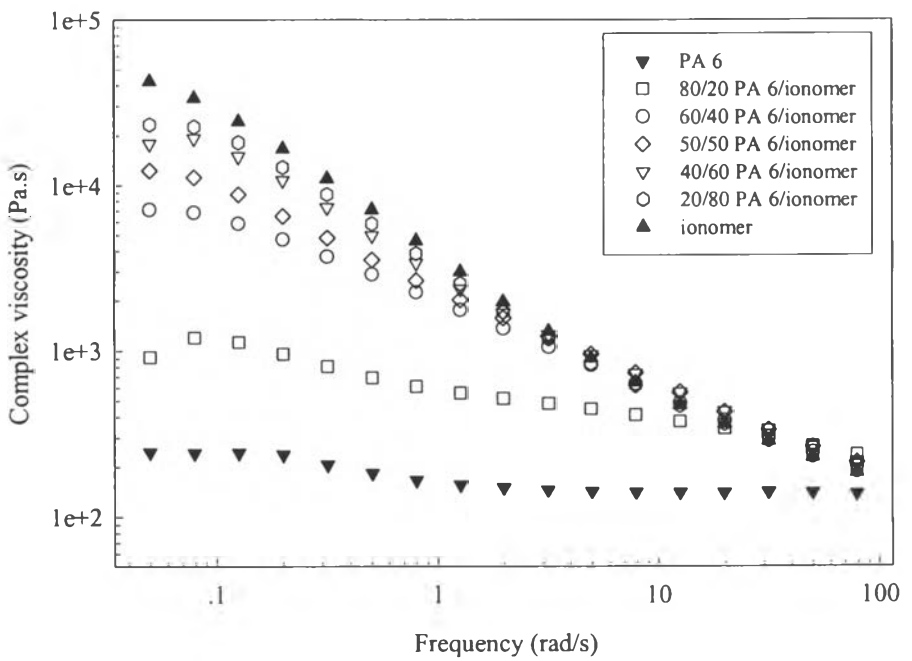

Figure 4.14 Complex viscosity, η^*, as a function of frequency for pure PA 6, pure ionomer and PA 6/ionomer blends.

The η^* of pure PA 6 is low and relatively constant over most of the experimental range. By contrast, the η^* value of pure ionomer did not reach a constant value but continued to decrease with increasing frequency. This could be ascribed to the strong self-aggregation of the ionic groups, which leads to ionic network formation.

The composition dependence of blends on viscoelastic functions gives much information about the degree of miscibility of the blended material. For miscible blends, viscoelastic functions usually follow the log-additivity rule:

$$\log F_b = \phi_m \log F_m + \phi_d \log F_d$$

where F is a viscoelastic function, ϕ is volume fraction, and subscripts "b", "m" and "d" refer to the blend, the matrix and the dispersed phase, respectively. By contrast, viscoelastic functions for immiscible blends deviate from the log-additivity rule. Immiscible polymer blends can be classified into three categories depending on the blend composition dependence of viscoelastic functions. These categories are (i) positive deviation, (ii) negative deviation, and (iii) positive/negative deviation, depending on whether the deviation from log-additivity is positive, negative or both for different composition regions (Yashikawa *et al.*, 1994).

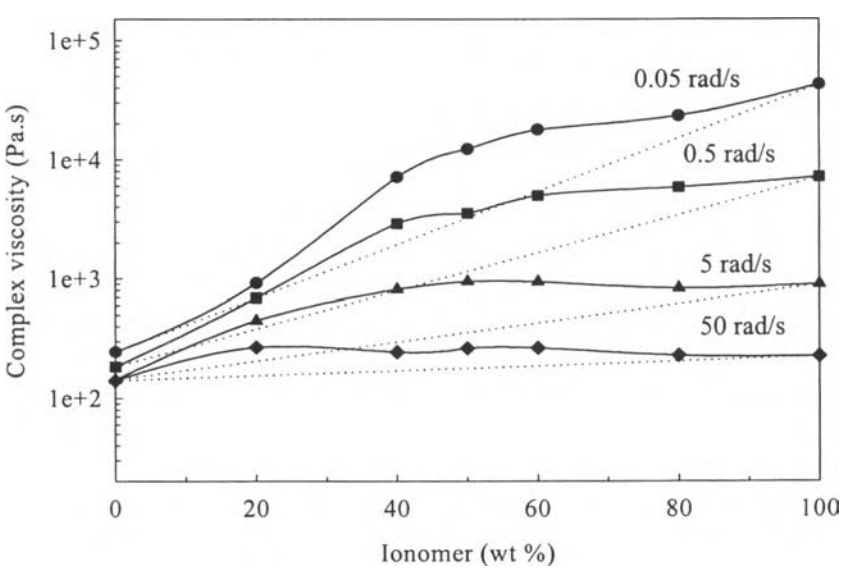

Figure 4.15 Complex viscosity, η^*, as a function of blend composition for PA 6/ ionomer blends at various frequencies.

Figure 4.15 shows the η^* of PA 6/ionomer blends at various frequencies as a function of the ionomer content. η^* of PA 6/ionomer blends showed deviations from the log-additivity rule (represented by the broken lines). Only positive deviations were observed. The magnitude of these deviations increased as the frequency decreased. This suggests that PA 6/ionomer blends are immiscible.

4.2.3.2 Viscoelastic Behavior

Many experimental studies have been made on the linear viscoelastic behavior of immiscible blends. It is generally observed that this behavior is characterized by an additional relaxation process at low frequencies, due to the dispersed phase deformation during oscillatory shear.

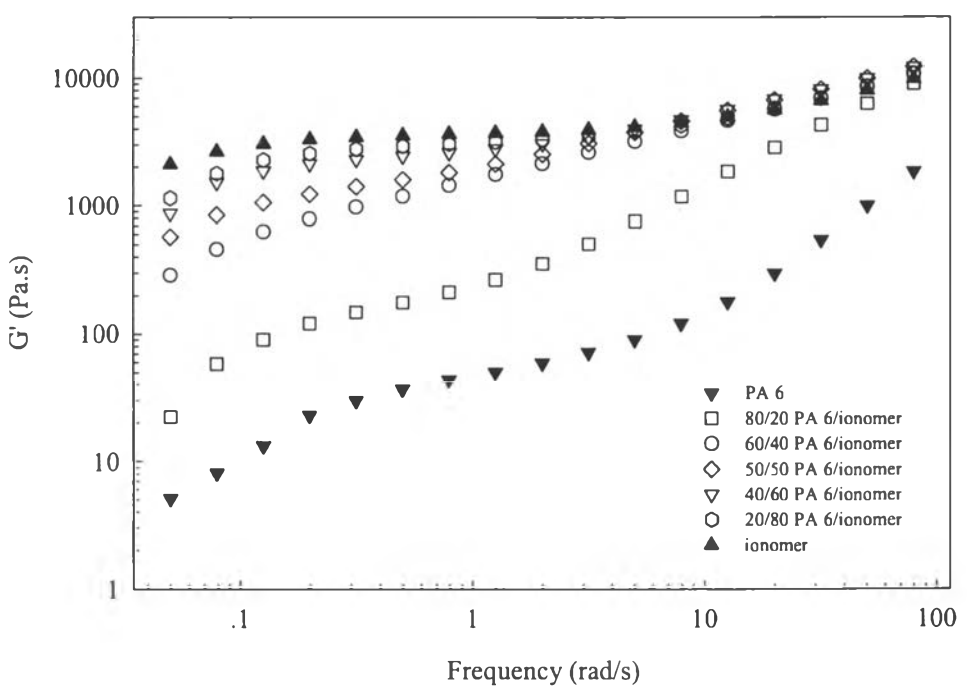

Figure 4.16 Storage moduli, G', as a function of frequency for pure PA 6, pure ionomer and PA 6/ionomer blends.

The storage modulus, G', represents the elastic response of the material, related to the potential energy stored by the material. Under deformation and at low frequencies G' is sensitive to macroscopic structure formation. Thus, it is worthwhile to compare the G' of the blends to the G' of the pure materials. Figure

4.16 shows G' curves for PA 6/ionomer blends as a function of frequency. It was found that G' values of all the blends lay between the G' values of the pure PA 6 and pure ionomer. All G' values increased with increasing ionomer content.

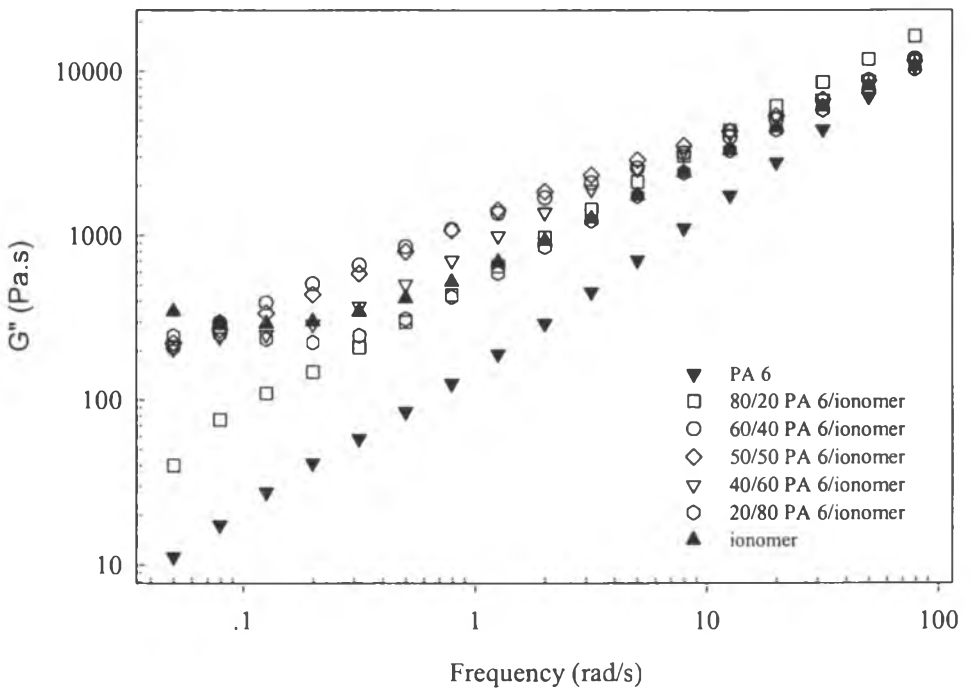

Figure 4.17 Loss moduli, G", as a function of frequency for pure PA 6, pure ionomer and PA 6/ionomer blends.

Loss modulus, G", is the viscous response of the material. This parameter represents the dissipation of energy as heat during deformation. Figure 4.17 shows G" curves as a function of frequency for PA 6/ionomer blends. It was found that with increasing ionomer content G" increased and the values were always higher than pure PA 6. It is proposed that chemical interactions occurred in these blends to give graft copolymers which therefore contain more long chain branches. The long chain branching will increase the viscous behavior and result in greater dissipation of energy.

At low frequencies, 0.05-0.2 rad/s, it was noticed that G" values for pure ionomer and the blend containing 80 % ionomer increased with decreasing

frequency. This curve bending is ascribed to the formation of a thermolabile network of ionic groups in the ionomer (Yoshikawa *et al.*, 1994).

4.2.4 Differential Scanning Calorimetry

Figure 4.18 displays DSC melting thermograms of pure PA 6, pure ionomer and PA 6/ionomer blends. For pure PA 6 and PA 6-rich blends, two melting peaks of PA 6 at 215 °C and 222 °C were observed. It has been reported (Weeding *et al.*, 1988; Galeski *et al.*, 1991) that PA 6 has two kinds of crystalline structure, a monoclinic α-form crystalline structure having a melting temperature of 221 °C and a γ-form having a melting temperature of 215 °C. Thus, it is clear from Figure 4.18 that the presence of ionomer caused the γ-form melting peaks of PA 6 to disappear. On the other hand, the melting temperature of pure ionomer was 94 °C and the characteristic peak was observed in all PA 6/ionomer blends. The ionomer melting temperature of blends was little affected by the presence of PA 6.

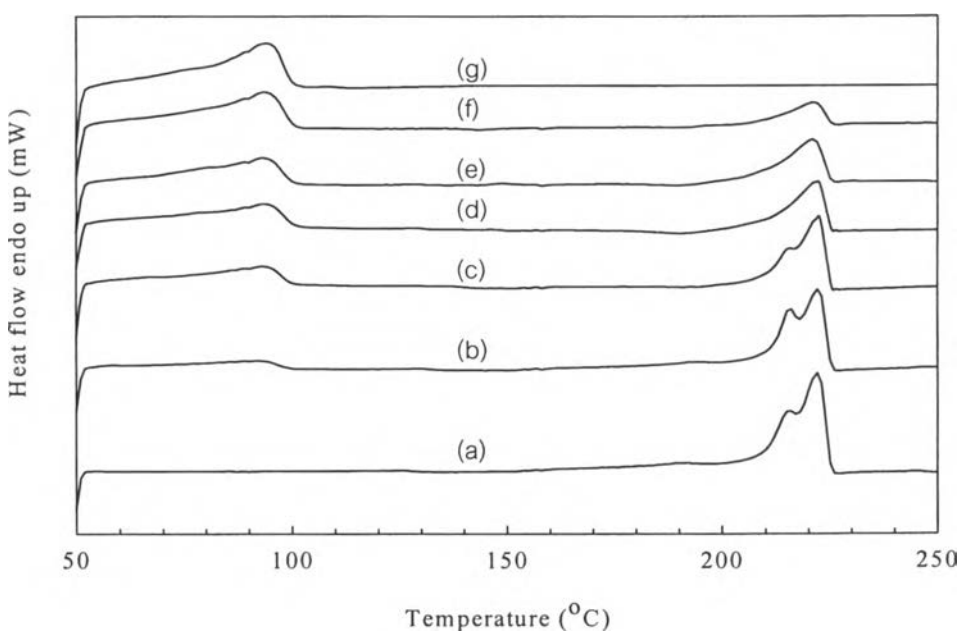

Figure 4.18 DSC melting thermograms of PA 6/ionomer blends: (a) 100/0, (b) 80/20, (c) 60/40, (d) 50/50, (e) 40/60, (f) 20/80, (g) 0/100.

Figure 4.18 shows that the PA 6 and ionomer components of the blends melt separately and are sufficiently far apart to enable the percentage crystallinity of each component in the blends to be calculated. (Section 3.1.4). The percentage weight fraction crystallinity of PA 6 and ionomer in PA 6/ionomer blends, as a function of ionomer content, are shown in Figure 4.19.

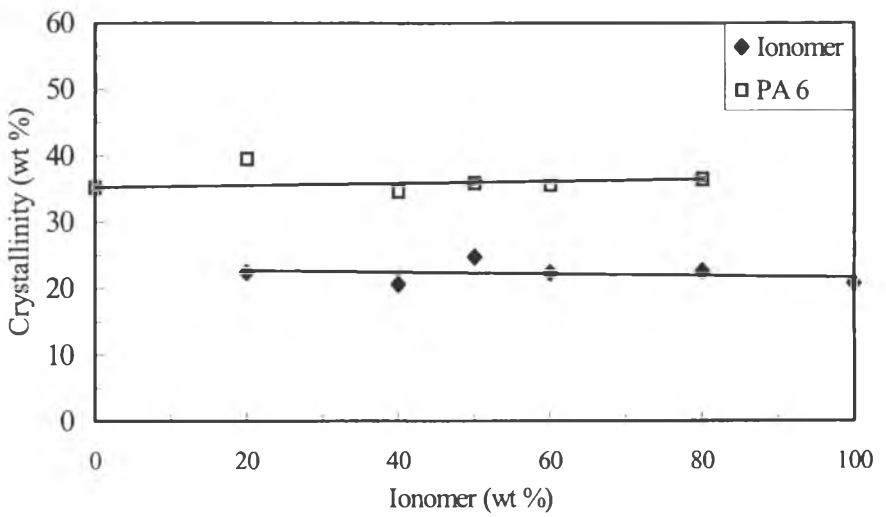

Figure 4.19 Percentage weight fraction crystallinity of PA 6 and ionomer in PA 6/ ionomer blends as a function of ionomer content, calculated from DSC melting peak areas.

The weight fraction crystallinity of both PA 6 and ionomer in the blends were quite constant and equal to pure PA 6 and ionomer respectively. There were differences of only $\pm$ 1.7 % for PA 6 and $\pm$ 1.5 % for ionomer. This suggests that crystallinity of one component of the blend is little affected by the presence of the other component.

The crystallization temperatures (T_c) of PA 6 and ionomer in PA 6/ ionomer blends are presented in Figure 4.20. The T_c peak of pure PA 6 occurred at 192 ^{o}C. There was no change in the T_c of PA 6 in the blends. However, T_c peaks of PA 6 could not be observed in the ionomer-rich blends. This indicated that the ionomer interfered with the crystallization of PA 6 in these blends. In contrast, T_c of ionomer for all PA 6/ionomer blends were significantly shifted to higher temperatures which suggests that PA 6 behaves as a nucleating agent for the

ionomer. Table 4.6 summarizes the DSC data of the PA 6/ionomer blends and pure polymers.

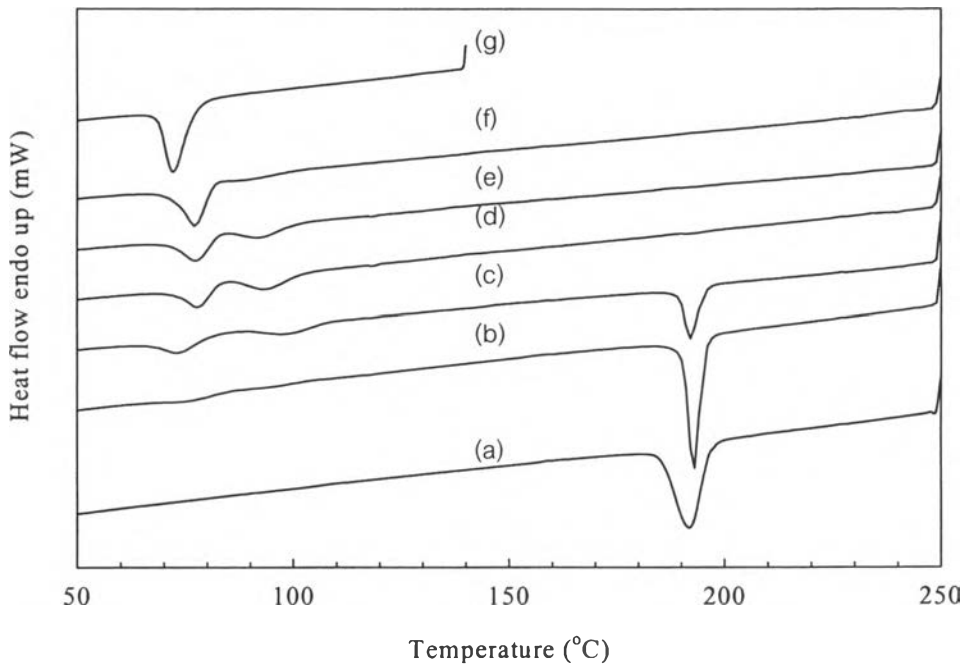

Figure 4.20 DSC crystallization thermograms of PA 6/ionomer blends: (a) 100/0, (b) 80/20, (c) 60/40, (d) 50/50, (e) 40/60, (f) 20/80, (g) 0/100.

Table 4.6 Crystalline properties of PA 6 and ionomer in PA 6/ionomer binary blends as determined by DSC

Blend composition (PA 6/ionomer)	PA 6 crystallites				Ionomer crystallites		
	T_m (°C)		T_c (°C)	Crystallinity (%)	T_m (°C)	T_c (°C)	Crystallinity (%)
	T_m^{α}	T_m^{γ}					
100/0	222.0	215.7	191.9	35.2	-	-	-
80/20	222.3	215.7	192.7	39.5	92.2	75.2	22.4
60/40	222.3	215.3	192.0	34.6	93.2	73.3	20.6
50/50	221.8	-	-	35.8	93.6	77.8	24.7
40/60	221.0	-	-	35.6	93.5	77.4	22.3
20/80	221.4	-	-	36.4	93.7	77.2	22.5
0/100	-	-	-	-	94.0	72.2	20.7

4.2.5 X-ray Diffraction

WAXS analysis was performed in order to study the crystalline structure of the blends and relate them to their compositions. WAXS patterns of PA 6/ionomer blends and pure components are presented in Figure 4.21.

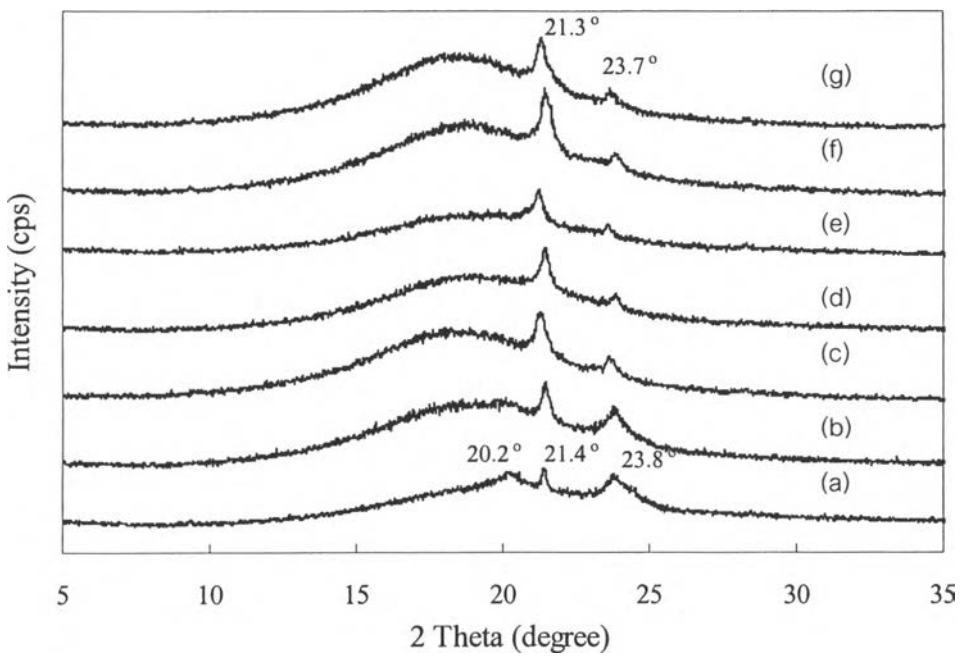

Figure 4.21 WAXS patterns of PA 6/ionomer blends: (a) 100/0, (b) 80/20, (c) 60/40, (d) 50/50, (e) 40/60, (f) 20/80, (g) 0/100.

The WAXS pattern for pure PA 6 gave pronounced peaks at $2\theta = 20.2^{\circ}$, 21.4° and 23.8°. The WAXS peaks at 20.2° and 23.8° are associated with the crystalline α_1-form and α_2-form structures, respectively and at 21.4° the γ-form crystal structure (Weeding *et al.*, 1988; Galeaski *et al.*, 1991). For pure ionomer, two pronounced peaks at $2\theta = 21.3^{\circ}$ and 23.7° were observed. The WAXS spectra peaks at 21.3° and 23.7° were in the (110) and (200) directions respectively and were ascribed to be orthorhombic crystal structures (Psarski *et al.*, 2000).

For PA 6/ionomer blends, the WAXS patterns gave only two distinct peaks ($2\theta = 21.4^{\circ}$ and 23.8°) which were also observed in both pure PA 6 and ionomer. However, it is proposed that there are both α_2- and γ-forms of PA 6, and an orthorhombic crystal structure of ionomer present in the PA 6/ionomer blends. This

proposal was confirmed from DSC results in which two separate, clearly defined melting peaks of PA 6 and ionomer were observed and the T_ms were unchanged for all blend compositions. In other words, the PA 6 and ionomer crystallize independently of each another and indicates that no interactions occur between the crystalline phases of PA 6 and ionomer.

In addition, it was noticed that the γ-form crystal structure, which could not be observed for all PA 6/ionomer compositions by DSC, was observed for all compositions by WAXS. However, no PA 6 peak at $2\theta = 20.2^{\circ}$ (α_1-form crystal structure) could be observed for blends containing ionomer because the crystallites would be covered by the amorphous phase in the blends.

4.2.5 Mechanical Properties

4.2.6.1 Tensile Properties

Mechanical properties, in terms of tensile strength, elongation at break and tensile modulus, for pure PA 6, pure ionomer and all of the blends are summarized in Table 4.7. All PA 6/ionomer blends showed lower tensile strength, elongation at break and tensile modulus compared with pure PA 6. In particularly, the tensile strength and tensile modulus decreased with increasing ionomer content. The elongation at break for all blends were much lower than for pure PA 6 and pure ionomer. This effect can be explained with reference to the tensile fracture mechanism which occurs in two-phase polymeric systems.

It has been widely accepted that in such systems the particles of the dispersed phase act as stress concentrators, introducing weak points in the materials. As a result, an intrinsically tough matrix breaks at lower stress, at lower elongation and at lower modulus compared with a material free of these particles. At the same time, however, an isolated crack can rapidly propagate through the pure polymer matrix with only a small amount of fracture energy. But if a large number of cracks are present, their stress fields can interfere when they pass near one another. Chemical interaction occurring within these blends could strongly reduce the stress at the tips of the cracks and could stop their growth and give more compatibility, so elongation at break should be higher (MacKnight *et al.*, 1985).

Table 4.7 Ultimate tensile properties of PA 6/ionomer binary blends

Blend composition (PA 6/ionomer)	Tensile strength (MPa)	Elongation at break (%)	Tensile modulus (MPa)
100/0	67.7 ± 4.7	288.9 ± 18.7	2479.4 ± 415.9
80/20	45.1 ± 0.3	24.9 ± 5.0	2013.6 ± 171.5
60/40	23.3 ± 1.0	9.3 ± 2.0	1269.2 ± 173.0
50/50	20.6 ± 0.5	27.5 ± 3.7	1081.2 ± 362.1
40/60	19.6 ± 0.4	67.8 ± 24.5	1150.5 ± 330.5
20/80	17.8 ± 1.1	187.6 ± 57.2	833.3 ± 261.9
0/100	17.9 ± 1.0	327.8 ± 22.8	528.0 ± 51.3

As mentioned above, there were no loosely attached dispersed domains observed in the matrix (see SEM micrographs). However, the "stress-concentration" actions of the domains could account for the lowering of the mechanical properties of PA 6 on blending with ionomer.

4.2.6.2 *Izod Impact Properties*

Izod impact properties of PA 6 and PA 6/ionomer blends are shown in Figure 4.22. The impact strength of PA 6 dramatically improved with increasing ionomer content. Since the blends contained large amounts of ionomer (more than 50 % by weight), the characteristically high impact strength of the ionomer was dominant. Thus, none of the samples having high ionomer content broke during impact testing. This result can be explained in terms of the T_gs of the PA 6 and ionomer. The T_g of PA 6 is above room temperature, i.e. the temperature of testing. So PA 6 gave a brittle response, or low impact strength value. However, when blending PA 6 with ionomer, lower T_g values for PA 6 peaks were obtained. This was because the high impact strength of the rubbery component of the PA 6/ionomer blends raised the impact strength of the PA 6/ionomer blend.

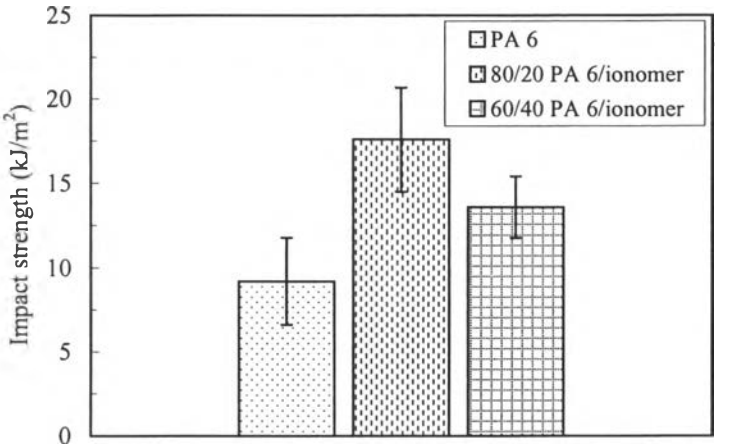

Figure 4.22 Izod impact properties of pure PA 6 and PA 6/ionomer blends.

In addition, since chemical interaction occurred at the interface of the PA 6/ionomer blends, the absorbed energy could be transferred from one phase to the other. Thus, higher impact strengths were obtained.

Furthermore, it was noticed that the impact strength value of the 60/40 PA 6/ionomer blend showed a slight drop from what was expected; it was expected that the impact strength should continuously increase with increasing ionomer content. This result may be explained in terms of phase inversion, i.e. the ionomer became the continuous phase with large globule aggregations of PA 6 contained within it (see Figure 4.12 b). This phase inversion causes the impact strength to become poorer. The causes of phase inversion are: (i) the component with the lower melt viscosity tends to encapsulate the higher viscosity material (ii) mismatch in the melt viscosities of the components causing the minor component to become the continuous phase (Kudva *et al.*, 1999). This certainly appeared to be the case here. The complex viscosity of ionomer is larger than that of PA 6 (section 4.2.3.1).

4.2.6.3 Hardness

Shore D hardness values of pure PA 6, pure ionomer and PA 6/ ionomer blends as a function of ionomer content are shown in Figure 4.23. PA 6 gave higher hardness (82) than pure ionomer (60). The higher hardness is related to

the higher crystallinity of PA 6, as observed from DSC studies. The hardness of PA 6/ionomer blends decreased with increasing ionomer content. This could be attributed to the softening effect due to the ionomer content. However, the hardness of the blends varied only slightly with blend composition. These results are in agreement with the almost constant degree of crystallinity found for all blends (section 4.2.4).

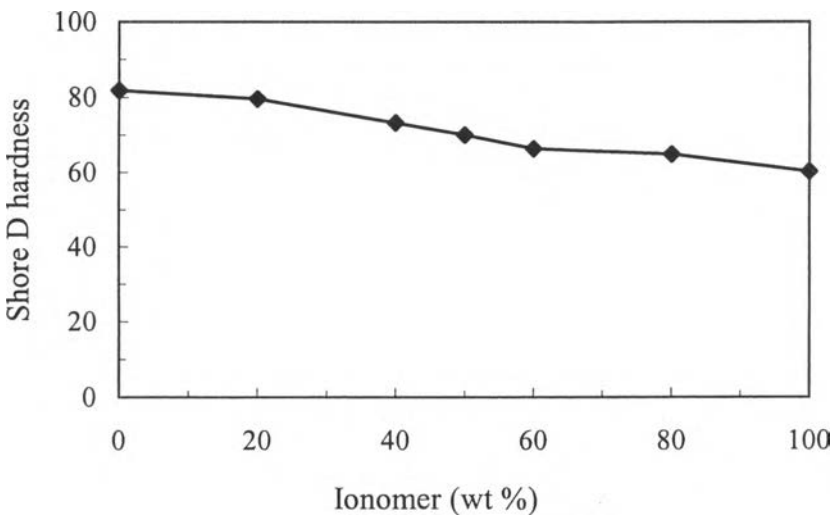

Figure 4.23 Shore D hardness of pure PA 6, pure ionomer and PA 6/ionomer blends as a function of ionomer content.

4.2.7 Surface Gloss

Gloss is one of the dominant properties of ionomers, so high gloss values were expected for the PA 6/ionomer blends. However, as the results in Figure 4.24 show, gloss values decreased with increasing ionomer content (up to 60 % by weight). It is proposed that the poor gloss might be caused by the cooling step during sample preparation by compression molding. During this step, the specimens were cooled down from 250 °C to 50 °C over a period of 10 min. This slow cooling rate could allow a large number of crystals to form. In general, the more homogeneous the material, the higher the surface gloss. Thus a large number of crystals would create heterogeneity in the material and therefore give lower gloss than would be expected for the semi-crystalline samples prepared.

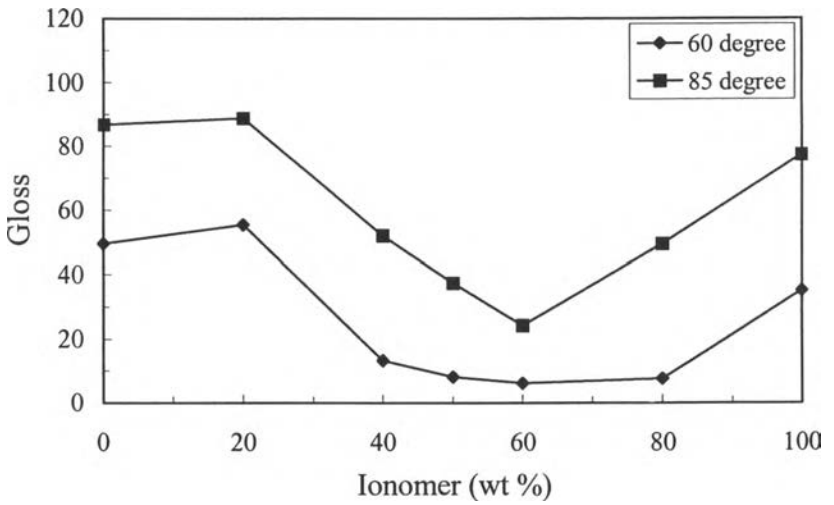

Figure 4.24 Surface gloss measured at 60 ° and 80 ° reflectance angles for pure PA 6, pure ionomer and PA 6/ionomer blends as a function of ionomer content.